Available online at www.CivileJournal.org

Civil Engineering Journal

(E-ISSN: 2476-3055; ISSN: 2676-6957)

Vol. 11, No. 06, June, 2025

Advancing Seismic Performance: Experimental Behavior of Hybridized Steel-FRP Composite Bars

Mohamed H. Agamy [1*], Ahmed Gouda [1, 2], Ibrahim T. Mostafa [1, 3], Omar F. Nassar [1], Heba Mohamed EL Said Issa [4], Ahmed M. Ahmed [1, 5]

[1] *Department of Civil Engineering, Faculty of Engineering, Helwan University (HU), Cairo 11795, Egypt.*

[2] *Department of Civil and Environmental Engineering, Faculty of Engineering, King Abdulaziz University (KAU), Jeddah, Saudi Arabia.*

[3] *Department of Civil and Building Engineering, University of Sherbrooke, Quebec, Canada.*

[4] *Housing and Building National Research Center-Reinforced Concrete Institute (HBRC), Cairo, Egypt.*

[5] *Civil and Construction Engineering, School of Engineering and Applied Science, Nile University, Giza, Egypt.*

Received 04 March 2025; Revised 19 May 2025; Accepted 26 May 2025; Published 01 June 2025

Abstract

This study investigates the structural performance of reinforced concrete (RC) columns reinforced with hybrid Steel-FRP Composite Bars (SFCBs), offering a sustainable alternative to conventional steel and fiber-reinforced polymer (FRP) reinforcement. Eight large-scale RC columns, measuring 400 × 400 mm in cross-section and 1850 mm in height, were tested under combined cyclic and axial loading to simulate seismic conditions. The experimental variables included SFCB diameters (14 mm, 18 mm, 22 mm), axial load ratios (20%, 30%, 40%), and stirrup spacing (80 mm, 100 mm, 150 mm). The results indicate that SFCBs can effectively replace traditional steel reinforcement, providing comparable load-bearing capacity while significantly improving durability. Columns reinforced with SFCBs demonstrated superior initial stiffness and achieved higher drift ratios than steel-reinforced columns, exceeding the limits set by international design codes (ACI 440.2R, CSA S806-12, Eurocode 8) with maximum drift ratios of up to 6.5%. Increasing the SFCB diameter from 14 mm to 22 mm enhanced peak load capacity by 14%–20% and improved drift ratios by up to 113%. However, higher axial load ratios and wider stirrup spacing were found to reduce ductility. Specifically, increasing the axial load ratio from 20% to 40% decreased ductility by 13.46%, while increasing stirrup spacing from 80 mm to 150 mm reduced ductility by 8.90%. These findings underscore the potential of SFCBs to enhance the performance of RC columns in seismic and corrosive environments, offering a durable and sustainable solution for modern infrastructure. To the authors' knowledge, this study represents the first comprehensive investigation into the behavior of SFCB-reinforced RC columns under combined cyclic and axial loading, providing valuable insights for the design of resilient concrete structures.

Keywords: Reinforced Concrete Columns; Cyclic Loading; Axial Load Ratio; Hybrid Reinforcement; SFCB; FRP; Stirrup Spacing; Seismic Performance.

1. Introduction

The structural integrity and durability of reinforced concrete (RC) structures are of paramount importance, particularly in environments prone to corrosion and seismic activity. Traditional steel reinforcement, while offering high tensile strength and ductility, is susceptible to corrosion in aggressive environments such as coastal regions and areas exposed to deicing salts. Corrosion-induced deterioration leads to reduced structural performance, increased

* Corresponding author: mohammedhelmy@m-eng.helwan.edu.eg

http://dx.doi.org/10.28991/CEJ-2025-011-06-018

maintenance costs, and shortened service life [1-3]. To mitigate these issues, Fiber Reinforced Polymers (FRPs), particularly Glass-FRP (GFRP), have been introduced as a corrosion-resistant alternative to steel reinforcement. GFRP possesses a high strength-to-weight ratio, excellent durability, and non-magnetic properties, making it a suitable option for RC structures exposed to harsh conditions. However, GFRP-reinforced members generally exhibit lower stiffness and limited ductility due to the material's low modulus of elasticity compared to steel, which raises concerns regarding their performance in seismic applications [4-7].

Numerous studies have examined the structural behavior of FRP-reinforced concrete elements. Windisch et al. [5] reported that while GFRP-reinforced beams exhibit superior corrosion resistance, they suffer from reduced ductility and energy dissipation under cyclic loading. Similarly, De Luca et al. [8] investigated the axial capacity of FRP-reinforced columns and found that while they perform adequately under lower axial loads, their brittleness leads to significant performance degradation under higher axial loads. Manalo et al. [6] further explored the long-term performance of GFRP reinforcement, emphasizing issues related to bond strength and durability.

To address the limitations of both steel and FRP reinforcements, hybrid reinforcement strategies have been proposed. One promising approach involves Steel-FRP Composite Bars (SFCBs), which combine a steel core with an FRP outer layer. This hybrid reinforcement seeks to capitalize on the high tensile strength and ductility of steel while maintaining the corrosion resistance of FRP. Research by Etman et al. [9] and Wu et al. [10] has demonstrated that SFCBs exhibit superior mechanical properties compared to conventional steel and FRP bars, making them particularly suitable for use in aggressive environments. Limited studies have focused on the seismic performance of hybrid-reinforced structures [11-14]. Sun et al. [11] and Huang et al. [12] examined the cyclic behavior of hybrid steel-FRP-reinforced concrete columns, highlighting their improved energy dissipation and ductility relative to FRP-reinforced columns. Additionally, Ge et al. [13] and Xu et al. [14] demonstrated that SFCB-reinforced columns exhibit enhanced fatigue resistance, ductility, and seismic performance, suggesting their viability in earthquake-resistant structures.

Despite these promising findings, research on the behavior of SFCB-reinforced RC columns under combined cyclic and axial loading remains limited. Most existing studies, such as Ali & El-Salakawy [15], have primarily focused on the seismic performance of GFRP-reinforced columns without extending their analyses to hybrid SFCB-reinforced members. Consequently, a comprehensive understanding of the load-carrying capacity, failure mechanisms, and deformation characteristics of SFCB-reinforced columns under seismic loading conditions is still lacking. This research aims to bridge this gap by experimentally investigating the structural response of SFCB-reinforced RC columns under combined axial and cyclic loading, with a focus on their load-deformation behavior, ductility, and failure mechanisms.

The remainder of this paper is organized as follows: Section 2 discusses the research significance and objectives. Section 3 details the experimental program, covering specimen preparation, testing procedures, and instrumentation. Section 4 presents the test results, emphasizing key findings on failure modes and load-displacement behavior. Sections 5 and 6 focus on the ductility and cumulative energy results of the columns, while Sections 7 and 8 provide additional discussions, including column rotation and reinforcement strains. Section 9 offers design recommendations based on various standards. Section 10 concludes the study. Finally, Sections 11 and 12 contain declarations and references, respectively. The flowchart that shows the methodology of the research is shown in Figure 1.

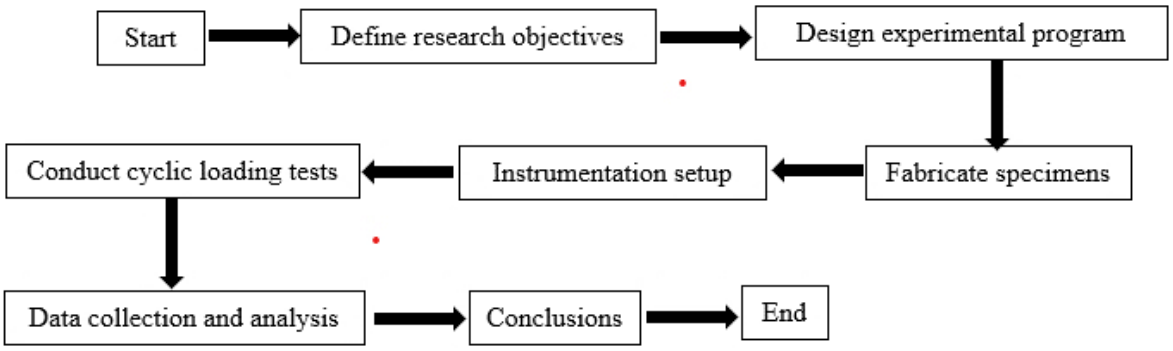

Figure 1. Methodology of the research

This study aims to bridge this gap by investigating the performance of SFCB-reinforced RC columns under combined cyclic and axial loading. The research focuses on evaluating the effects of key variables, including SFCB bar diameter, axial load ratio, and stirrup spacing, on structural behavior. The significance of this research lies in its potential to advance the understanding and application of hybrid reinforcement in concrete structures, particularly in

seismic zones. By addressing the limitations of traditional materials and offering a sustainable alternative, this study contributes to the development of more durable, resilient, and cost-effective construction practices. The primary objectives of this research are:

- To evaluate the performance of SFCB-reinforced RC columns under cyclic loading conditions, simulating seismic activity.
- To determine the influence of key variables, including SFCB bar diameter, axial load ratio, and stirrup spacing, on the structural behavior of these columns.
- To compare the performance of SFCB-reinforced columns with traditional steel-reinforced columns in terms of drift ratio, load capacity, and deflection characteristics.

To provide practical recommendations for the use of SFCBs in seismic-resistant concrete structures, supported by experimental data and analysis.

2. Experimental Program

2.1. Materials

3.1.1. Reinforcing Bars

The experimental program involved the testing of RC columns reinforced with SFCBs. For the hybrid reinforcement, three types of SFCBs were fabricated, each featuring a grade 400 steel core with a diameter of 10 mm. The steel core was encased in fiberglass layers of varying thicknesses (4 mm, 8 mm, and 12 mm), resulting in final bar diameters of 14 mm, 18 mm, and 22 mm, respectively. The manufacturing process for the SFCBs involved wrapping the steel core with glass fiber strings, placing them in epoxy-coated wooden molds, and immersing them in a vinyl-ester resin bath to ensure uniform coating and bonding. This process is illustrated in Figure 2. The mechanical properties of all reinforcement bars, including the modulus of elasticity and yielding tensile strength, were determined in accordance with the ASTM D7205 standard [16]. A reference column reinforced with conventional steel bars was also tested for comparison. The steel longitudinal reinforcement for the reference column consisted of No. 10M deformed steel bars. A summary of the mechanical properties is provided in Table 1, while Figure 3 presents the stress-strain curves for the SFCBs, highlighting their unique behavior under tensile loading.

(a) (b) (c) (d)

(e)

Figure 2. Manufacturing process of the hybrid bars; (a) 10 mm steel core with strain gauge; (b) Wooden form; (c) The steel core with fiber glass; (d) Compacting the wooden form; (e) The bars fully coated with the fiber glass

Table 1. Reinforcing Bars

Bars' type	Diameter (mm)	Area (mm²)	Elastic modulus (GPa)	Yielding strength (MPa)
SFCB	14.0	154	200.0	360
	18.0	254	165.0	284
	22.0	380	132.0	174
Steel	10.0	78.5	200.0	400

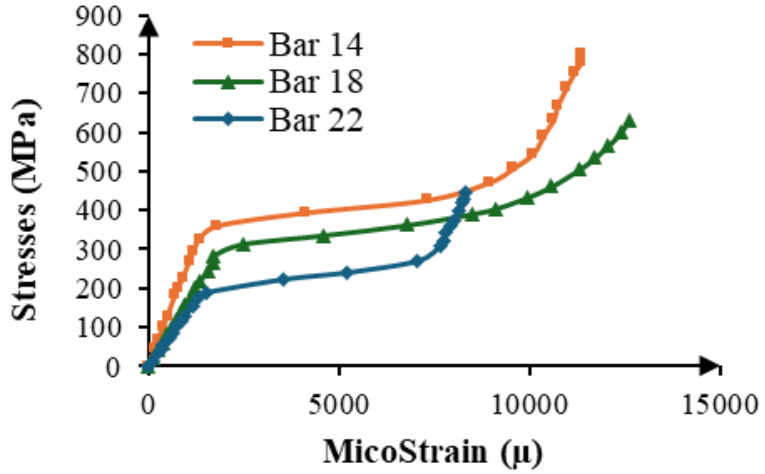

Figure 3. Stress-strain curve for the SFCB bars

3.1.2. Concrete

The concrete used for the columns was designed to achieve a target compressive strength of 35 MPa at 28 days. Pre-mixed concrete was procured from a local supplier to ensure consistency and quality. Prior to casting, the slump-flow of the concrete was measured to be between 500 and 600 mm, indicating adequate workability for the intended application. To verify the compressive strength of the concrete, tests were conducted on at least three standard cylindrical specimens (100 mm diameter × 200 mm height) in accordance with the ASTM C39/C39M standard [17]. The average compressive strengths of the columns, as determined from these tests, are summarized in Table 2 .Both the test cylinders and the columns were cured under identical conditions to ensure comparable strength development. In addition to compressive strength tests, split cylinder tests were performed on concrete specimens of the same dimensions (100 mm diameter×200 mm height) to evaluate the tensile strength. The results indicated an average tensile strength of approximately 3.2 MPa for the concrete used in the columns.

Table 2. Test Results

Column's ID	Compressive strength (MPa)	Max. drift ratio (%)	Max. lateral load (kN)	Ductility	Parameter investigated
					Steel core
S-10-80-20	35.0	2.2	79.20	5.00	Reference
F-14-80-20	35.0	2.6	121.7	5.33	GFRP thickness
F-18-80-20	34.5	5.6	142.8	5.75	
F-22-80-20	35.5	5.8	173.6	5.92	
F-18-80-30	36.0	6.1	143.1	5.25	% of vertical load
F-18-80-40	35.0	6.5	148.5	5.00	
F-18-100-20	35.5	5.5	137.1	5.50	Stirrups' spacing
F-18-150-20	36.5	6.0	140.7	5.25	

2.2. Details of Test Specimens

The primary objective of this study is to replace the flexural steel reinforcement in conventional RC columns with hybrid Steel-FRP Composite Bars (SFCBs) while maintaining comparable strength and performance. To achieve this, the behavior of hybrid RC columns was evaluated by systematically varying the following key parameters:

- *Bar Diameter*: The SFCBs consisted of a 10 mm diameter steel core wrapped with glass fibers of varying thicknesses (4 mm, 8 mm, and 12 mm), resulting in final bar diameters of 14, 18, and 22 mm, respectively. This variation allowed for an assessment of the influence of bar diameter on column performance.
- *Vertical Axial Load*: The axial load ratio, a critical parameter in column design, is defined as $P/fc'Ag$, where P is the applied axial load, fc' is the compressive strength of the concrete, and Ag is the gross cross-sectional area of the column. To study its effect, axial load ratios of 20%, 30%, and 40% of the column's maximum capacity were applied.
- *Stirrup Spacing*: The spacing of transverse reinforcement (stirrups) along the column height was varied at 80 mm, 100 mm, and 150 mm to investigate its impact on the column's behavior under cyclic loading.

Each test specimen represented a typical building column with a cross-sectional dimension of 400 × 400 mm and a height of 1850 mm. The columns were anchored to a reinforced concrete footing measuring 1200 × 600 mm in plan and 600 mm in height. The test program included one control column reinforced with traditional steel bars and seven columns reinforced with SFCBs. Cyclic loading tests were conducted to simulate seismic conditions, enabling an evaluation of crack propagation, load-carrying capacity, and deflection behavior. Figure 4 illustrates the dimensions and reinforcement details of a typical column.

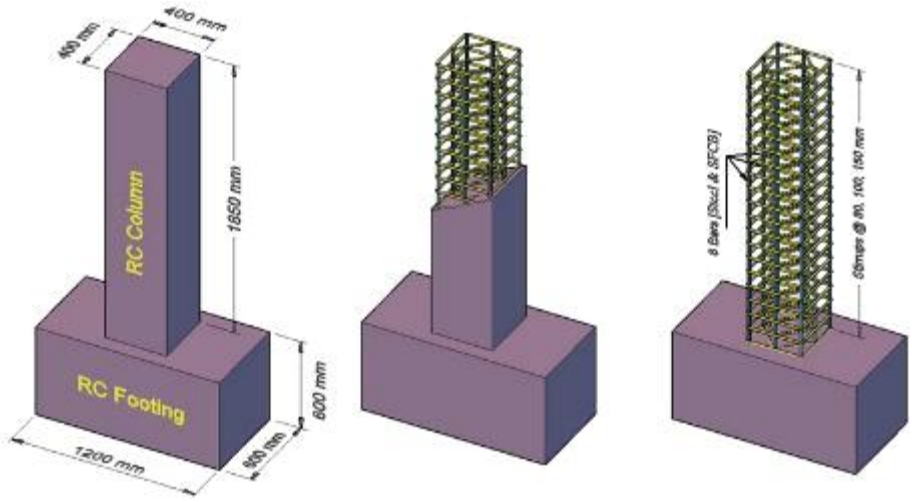

Figure 4. Concrete dimensions and reinforcement details (all dimensions are in mm)

Each column was assigned a four-character identifier:

- The first character indicates the type of flexural reinforcement: "S" for steel and "F" for SFCB.
- The second character represents the diameter of the flexural reinforcement.
- The third character denotes the stirrup spacing.
- The fourth character specifies the percentage of vertical axial load applied.

Detailed information about all columns is provided in Table 3. The test matrix included the following specimens:

- **S-10-80-20**: A control column reinforced with 8 - 10M steel bars, 80 mm stirrup spacing, and a 20% axial load ratio.
- **F-14-80-20**, **F-18-80-20**, and **F-22-80-20**: Columns reinforced with 14 mm, 18 mm, and 22 mm SFCBs, respectively, with 80 mm stirrup spacing and a 20% axial load ratio.
- **F-18-80-30** and **F-18-80-40**: Columns reinforced with 18 mm SFCBs, 80 mm stirrup spacing, and axial load ratios of 30% and 40%, respectively.
- **F-18-100-20**: A column reinforced with 18 mm SFCBs, 100 mm stirrup spacing, and a 20% axial load ratio.
- **F-18-150-20**: A column reinforced with 18 mm SFCBs, 150 mm stirrup spacing, and a 20% axial load ratio.

This systematic variation in reinforcement diameter, stirrup spacing, and axial load ratio allowed for a comprehensive evaluation of the structural performance of hybrid RC columns under cyclic loading conditions.

Table 3. Specimens Details

Column's ID	Column's dimensions (mm)	No. of bars	Bar's diameter (mm)		Total bar's diameter (mm)	Stirrups' spacing (mm)	Vertical load (%)
			Steel core	GFRP rapped			
S-10-80-20	400 by 400	8	10	-	10	80	20
F-14-80-20				4	14	80	20
F-18-80-20				8	18	80	20
F-22-80-20				12	22	80	20
F-18-80-30				8	18	80	30
F-18-80-40				8	18	80	40
F-18-100-20				8	18	100	20
F-18-150-20				8	18	150	20

2.3. Instrumentations

The structural behavior of the columns was meticulously monitored using a combination of electrical strain gauges and linear variable differential transformers (LVDTs). Six electrical strain gauges were carefully attached to both the longitudinal and transverse reinforcement at three distinct levels along the column height. These gauges were used to measure the strain distribution in the reinforcement under applied loads, providing critical insights into the stress response of the materials. LVDTs were employed to measure both local and global deformations. Three sets of LVDTs were strategically positioned on the column faces perpendicular to the loading direction within the plastic hinge region. These LVDTs were used to capture curvature changes, which are essential for understanding the column's flexural behavior under cyclic loading. Additionally, several LVDTs were installed at various heights along the columns to record lateral deformations, enabling a comprehensive assessment of the overall structural response.

2.4. Test Setup

The experimental setup for evaluating the RC columns under cyclic loading comprised a hydraulic actuator with a capacity of 1000 kN and a displacement range of ±250 mm, securely mounted within a robust steel reaction frame. A hydraulic jack was employed to apply a constant vertical load at the top of the column, simulating real-world axial stress conditions throughout the test. The cyclic lateral load was applied using the hydraulic actuator, with the applied force precisely measured by a 1000 kN load cell. To ensure uniform load distribution and stability, the column was supported by cylindrical drive plates and rotated loading plates. Critical points in the setup were reinforced with 25 mm thick steel plates (600 × 450 mm) and 10 mm thick stiffener plates to maintain structural integrity and prevent deformation during testing. Additional reinforcement was provided by six 25 mm diameter steel rods and 30 × 30 mm angle sections, each 400 mm in length, strategically placed to reinforce high-stress areas and prevent structural failure. The test setup is illustrated in Figure 5.

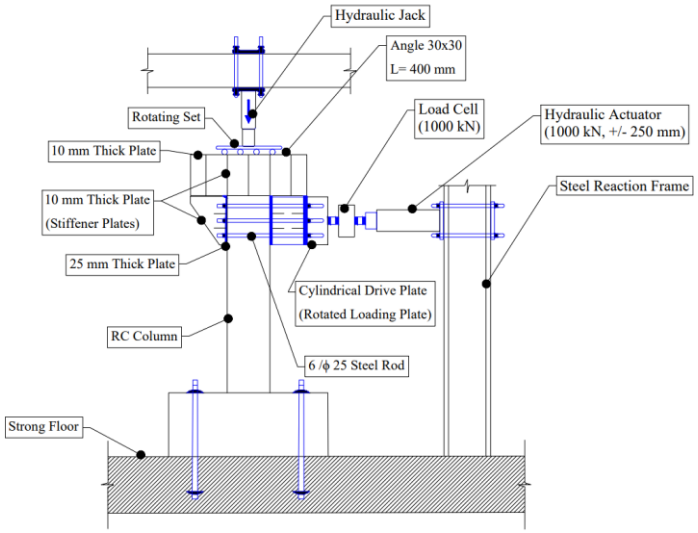

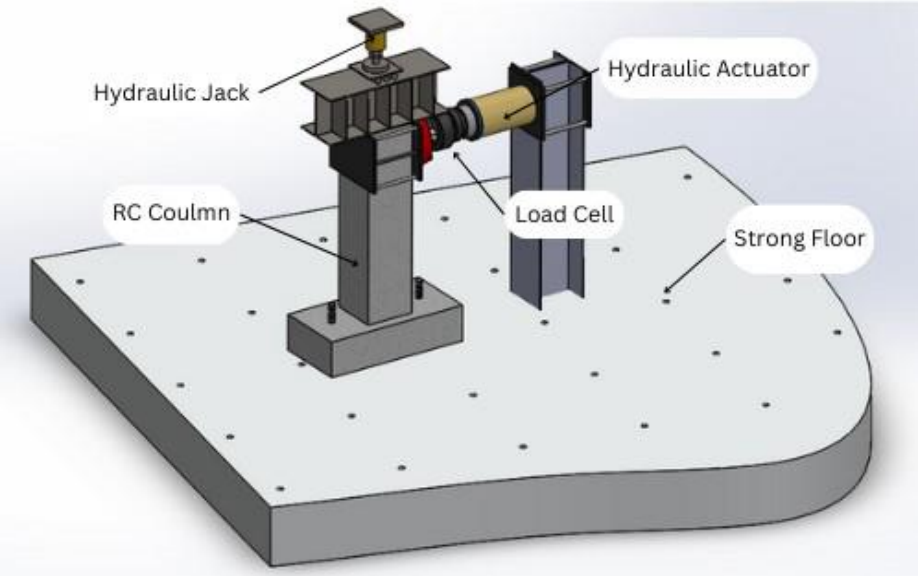

Figure 5. Test setup

The design of the setup ensured accurate load application and measurement while maintaining the stability of the reaction frame and other components. The testing procedure adhered to FEMA guidelines, as outlined in Figure 6. The process involved an initial preloading phase to stabilize the system, followed by cyclic loading with progressively increasing amplitudes until failure occurred. The loading rate was maintained at 1.5 mm/min to ensure controlled and consistent testing conditions. This setup effectively replicated real-world loading scenarios, providing reliable data on the performance of RC columns under cyclic loading. The results are critical for understanding the structural behavior of these columns and improving design standards for seismic-resistant structures.

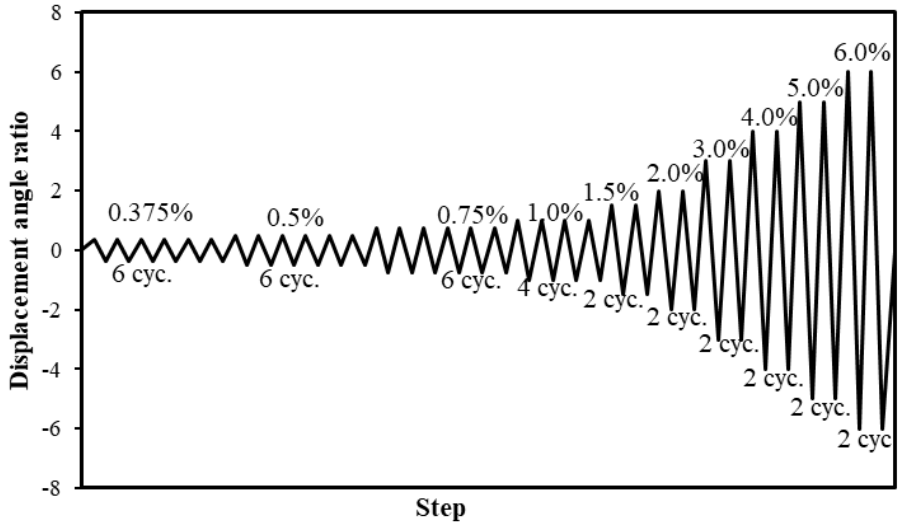

Figure 64. Loading steps (recreated from FEMA guidelines)

3. Results and Discussions

3.1. Crack Patterns

The lateral load-drift behavior of the eight columns is illustrated in Figure 7, while Figure 8 depicts their cracking patterns and failure modes. All columns exhibited a balanced lateral load-drift relationship during cyclic loading in both directions until concrete crushing occurred on one side. The response remained predominantly linear-elastic up to the initial cracking point, with SFCB-reinforced columns demonstrating higher initial stiffness compared to steel-reinforced columns. After the onset of cracking, all columns primarily exhibited a flexural response, characterized by horizontal cracks parallel to the rectilinear ties. In well-confined columns (F-14-80-20, F-18-80-20, and F-22-80-20), horizontal cracks extended up to approximately 50% of the column's effective height. In contrast, columns with lower confinement (F-18-100-20 and F-18-150-20) exhibited cracks extending up to 40% of the effective height.

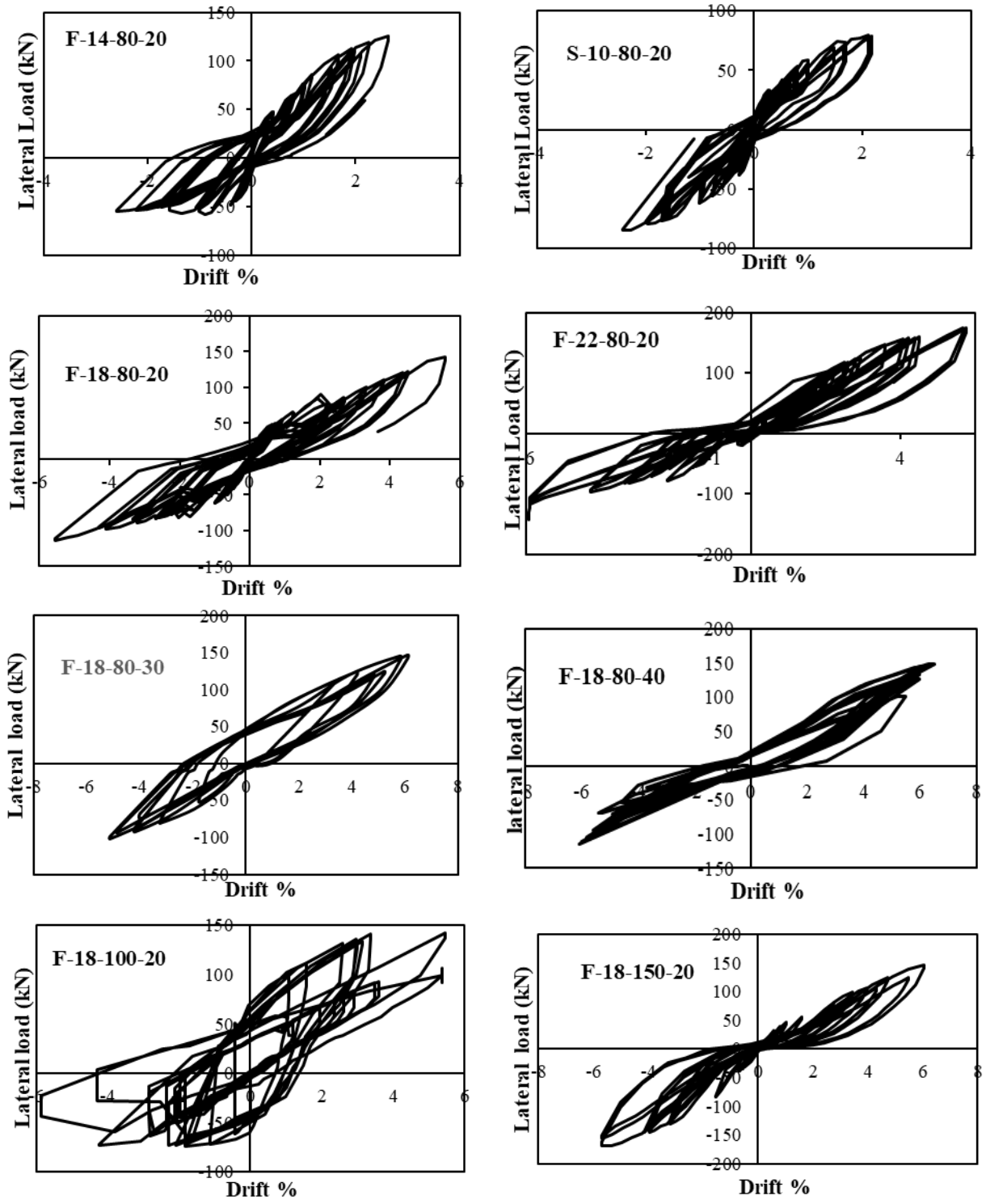

Figure 7. Load-drift response

During the initial loading phase, the steel bars in column S-10-80-20 yielded at a drift ratio of around 1.5%. As cyclic loading progressed, vertically splitting cracks typically appeared on the compressed side of both steel- and SFCB-reinforced columns. Concrete cover spelling became more pronounced beyond a lateral drift of 2.0% for all columns. In S-10-80-20, longitudinal bars buckled during the displacement cycle before concrete cover spalling. These buckled bars straightened under tension during the reversed load cycle, but the degradation in lateral resistance became more evident after the buckling of the outermost bars. Excessive buckling of steel bars was observed with further cyclic loading until the axial load was lost due to concrete core crushing. In contrast, SFCB-reinforced columns exhibited varying behaviors depending on test parameters. Columns with wider tie spacings (F-18-100-20 and F-18-150-20) experienced strength degradation before concrete cover spalling, while well-confined columns (F-18-80-20 and F-22-80-20) demonstrated a strength gain with a secondary peak. Columns with higher axial load ratios (F-18-80-30 and F-18-80-40) controlled the

strength gain but reached a plateau after the concrete cover spalled. The failure of the compressed longitudinal SFCB bars occurred at different drift levels, beginning at a minimum drift value of 2.6% for column F-14-80-20 and exceeding 5.4% drift for other SFCB-reinforced columns. These values are higher than the 2.5% minimum drift ratio recommended by many standards [1]. In contrast, the steel bars in column S-10-80-20 failed at an earlier drift level of 2.2%. The breakdown of the SFCB bars is depicted in Figure 7. As displacement increased, all columns lost axial load due to the crushing of the concrete core. The failure of SFCB-reinforced columns involved the rupture of the longitudinal SFCB bars. However, many columns, such as F-22-80-20, F-18-80-30, F-18-80-40, and F-18-150-20, reached the limit of the loading setup at close to 6.0% lateral drift. Figure 7 also shows the plastic hinge zone after the specimens failed.

Figure 8. Crack and failure mode

During the initial loading phase, the steel bars in column S-10-80-20 yielded at a drift ratio of around 1.5%. As cyclic loading progressed, vertically splitting cracks typically appeared on the compressed side of both steel- and SFCB-reinforced columns. Concrete cover spelling became more pronounced beyond a lateral drift of 2.0% for all columns. In S-10-80-20, longitudinal bars buckled during the displacement cycle before concrete cover spalling. These buckled bars straightened under tension during the reversed load cycle, but the degradation in lateral resistance became more evident after the buckling of the outermost bars. Excessive buckling of steel bars was observed with further cyclic loading until the axial load was lost due to concrete core crushing. In contrast, SFCB-reinforced columns exhibited varying behaviors depending on test parameters. Columns with wider tie spacings (F-18-100-20 and F-18-150-20) experienced strength degradation before concrete cover spalling, while well-confined columns (F-18-80-20 and F-22-80-20) demonstrated a strength gain with a secondary peak. Columns with higher axial load ratios (F-18-80-30 and F-18-80-40) controlled the strength gain but reached a plateau after the concrete cover spalled. The failure of the compressed longitudinal SFCB bars occurred at different drift levels, beginning at a minimum drift value of 2.6% for column F-14-80-20 and exceeding 5.4% drift for other SFCB-reinforced columns. These values are higher than the 2.5% minimum drift ratio recommended by many standards [1]. In contrast, the steel bars in column S-10-80-20 failed at an earlier drift level of 2.2%. The breakdown of the SFCB bars is depicted in Figure 7. As displacement increased, all columns lost axial load due to the crushing of the concrete core. The failure of SFCB-reinforced columns involved the rupture of the longitudinal SFCB bars. However, many columns, such as F-22-80-20, F-18-80-30, F-18-80-40, and F-18-150-20, reached the limit of the loading setup at close to 6.0% lateral drift. Figure 7 also shows the plastic hinge zone after the specimens failed.

The extent of damage was closely linked to the level of confinement: columns with larger tie spacing, lower confinement, and higher axial load ratios exhibited more extensive damaged areas. The damaged zone in all columns typically started around 50 mm above the base stub, primarily due to the additional confinement provided by the base stub to the column sections directly above it. Overall, columns with larger bar diameters and higher axial load ratios demonstrated superior load-drift performance and delayed buckling of the reinforcing bars. The load-drift responses indicate that these parameters significantly influence the structural integrity and deformation capacity of reinforced concrete columns. SFCB-reinforced columns outperformed those with traditional steel reinforcement, primarily due to the composite action of the SFCB bars, which provided better energy dissipation. These experimental results highlight the critical role of reinforcement type and configuration in determining the seismic resilience of concrete columns.

3.2. Steel vs. SFCB Reinforcement

A comparison between the steel-reinforced column (S-10-80-20) and the SFCB-reinforced column (F-14-80-20) highlights the significant advantages of using SFCB bars over traditional steel reinforcement. As shown in Figure 9-a, the SFCB-reinforced column demonstrated superior energy dissipation and delayed buckling, resulting in enhanced overall performance under cyclic loading. Specifically, the F-14-80-20 column achieved a peak lateral load increase of approximately 57% and a higher drift ratio of around 20% compared to the S-10-80-20 column. This improvement is attributed to the composite nature of SFCB bars, which combine the tensile strength of steel with the added benefits of fiber reinforcement. This combination leads to improved ductility and post-peak behavior, allowing the column to withstand greater deformations before failure. Additionally, the use of SFCB bars mitigated the early spalling of the concrete cover, preserving structural integrity for a longer duration and reducing the extent of post-failure damage. These findings underscore the potential of SFCB reinforcement to enhance the seismic performance of RC columns, offering a more resilient and durable alternative to traditional steel reinforcement.

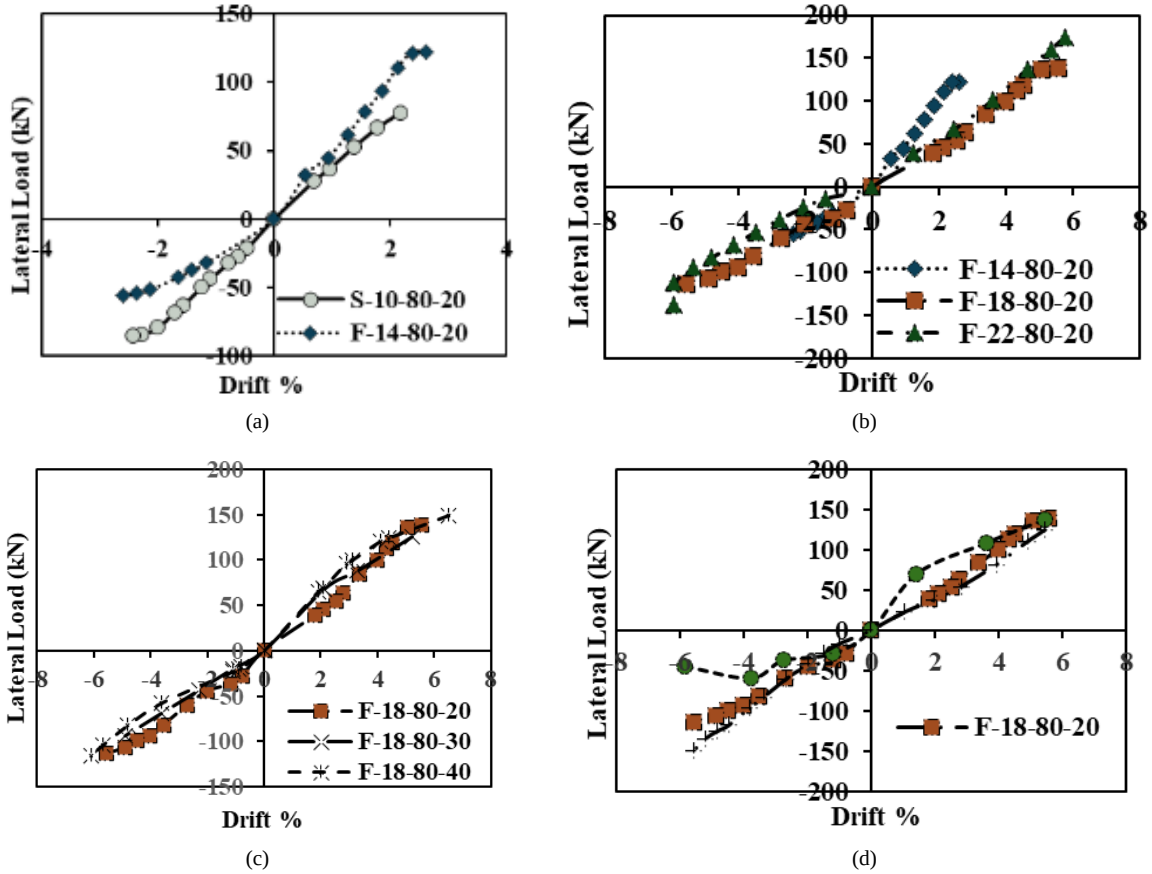

Figure 9. Failure envelope for all the specimens

3.3. Effect of SFCB Bar Diameter

The diameter of the SFCB bars had a significant influence on the performance of the columns, as illustrated in Figure 9-b. Columns F-14-80-20, F-18-80-20, and F-22-80-20, reinforced with SFCB bars of 14 mm, 18 mm, and 22 mm diameters, respectively, demonstrated progressively improved load-drift responses with increasing bar diameter. The F-18-80-20 column exhibited a 14% increase in peak load and a 113% higher drift ratio compared to F-14-80-20. The F-22-80-20 column further enhanced these performance metrics, achieving a 20% increase in peak load and a 4% higher drift ratio over F-18-80-20. Larger diameter bars provided a stronger bond with the surrounding concrete, enhancing structural integrity and delaying the onset of buckling. Additionally, the increased bar diameter contributed to better post-peak behavior, characterized by minimal cracking and the ability to sustain higher lateral loads before significant deformations occurred. These findings highlight the importance of selecting adequate reinforcement bar size in seismic design to ensure optimal structural performance and resilience.

3.4. Effect of Axial Load

In steel-RC columns, increasing the axial load typically reduces drift capacity due to higher compressive stresses in the concrete and reinforcement, resulting in a stiffer column with limited lateral deformation capability [1, 12]. However, in columns reinforced with SFCB bars, the response is more complex due to the combined properties of the steel core and FRP layers (Figure 9-c). While the steel core enhances stiffness, potentially reducing drift capacity under higher

axial loads, the FRP layers improve ductility and energy dissipation, partially offsetting the reduction in drift capacity observed in steel-reinforced columns [11–16]. The overall effect of axial load on the drift capacity of SFCB-reinforced columns depends on the balance between these opposing factors, as well as specific loading conditions. Key variables influencing this response include the ratio of steel to FRP content in the SFCB bars, the column's geometry, and the magnitude of the applied axial load [18, 19].

Columns F-18-80-20, F-18-80-30, and F-18-80-40, with axial load ratios of 20%, 30%, and 40%, respectively, demonstrated that higher axial loads led to increased peak lateral load capacity and drift ratio. Column F-18-80-30 exhibited a 3% higher peak load and a 9.5% increase in drift ratio compared to F-18-80-20. Similarly, column F-18-80-40 showed a 3.5% higher peak lateral load and a 6.5% higher drift ratio than F-18-80-30. These results are consistent with previous studies, which reported similar trends in CFRP-reinforced columns under higher axial loads [20]. For instance, a study on CFRP-RC columns with a 355-mm square cross-section tested under seismic conditions found that columns subjected to higher axial compression (33% of concentric load capacity) demonstrated a 25% increase in lateral force and a 50% higher drift ratio compared to those under lower axial loading (17% of concentric load capacity).

3.5. Effect of Ties Spacing

Increasing the spacing between ties in RC columns subjected to cyclic loading generally leads to higher drift, as illustrated in Figure 9-d. Ties provide lateral confinement to the concrete core, enhancing its strength and ductility. When tie spacing increases, this confinement effect diminishes, resulting in less restraint on the concrete core and higher lateral displacements or drift [21, 22]. Columns F-18-80-20, F-18-100-20, and F-18-150-20, with tie spacings of 80 mm, 100 mm, and 150 mm, respectively, demonstrated that tighter tie spacing improved confinement, delaying concrete cover spalling and reinforcing bar buckling. The F-18-100-20 column exhibited nearly the same peak lateral load, but a 5% higher drift ratio compared to F-18-80-20, due to the reduced confinement from wider tie spacing. Similarly, the F-18-150-20 column showed a 3% increase in peak lateral load and a 3.5% increase in drift ratio compared to F-18-100-20. These findings highlight the critical role of tie spacing in controlling the lateral deformation and overall performance of RC columns under cyclic loading. Closer tie spacing enhances confinement, improving the column's ability to resist lateral forces and maintain structural integrity during seismic events.

4. Ductility in RC-Columns

Ductility (μ) is a critical parameter in RC columns, defining their ability to undergo significant plastic deformation before failure. This characteristic is essential for energy dissipation during seismic events, as it allows structures to absorb and redistribute energy without sudden collapse. Ductility is typically expressed as the ratio of ultimate displacement (δ_u) to yield displacement (δ_y), as shown in Equation 1:

$$\mu = \frac{\delta_u}{\delta_y} \quad (1)$$

where δ_u is the displacement at the ultimate load, and δ_y is the displacement at the yield load.

In this study, the yield load was determined as the point where the load-displacement curve first deviated significantly from linearity, marking the onset of inelastic behavior. This was identified using a bilinear approximation of the envelope curve, where the intersection of the elastic slope and a line with reduced stiffness defined the yield load. The corresponding yield displacement was taken as the displacement at this load. This approach ensures an accurate representation of the transition from elastic to plastic behavior, accounting for the energy dissipation characteristics of the column under cyclic loading. High ductility is crucial for ensuring that structures can withstand significant deformation beyond their elastic limit, providing time for evacuation and reducing the risk of catastrophic failure during seismic events [23, 24].

4.1. Comparison of Ductility in Steel and SFCB-Reinforced Columns

The ductility of the SFCB-reinforced column F-14-80-20 was 5.33, representing a 6.60% increase compared to the steel-reinforced column S-10-80-20, which had a ductility of 5.00. This improvement indicated that the F-14-80-20 column exhibited enhanced deformation capacity, allowing it to sustain larger strains before reaching failure. The increased ductility implied a superior ability to dissipate energy under loading conditions, which is particularly beneficial in applications where structures are subjected to cyclic or seismic loads. This finding underscored the advantages of using SFCB reinforcement, as it contributed to greater structural resilience and improved performance compared to conventional steel reinforcement. The enhanced energy absorption capacity of the SFCB-reinforced column further suggested that it could provide better protection against sudden or progressive failure, making it a viable alternative for structures requiring high ductility and durability.

4.2. Effect of SFCB Bar Diameter on Ductility

A comparison of the hybrid columns F-14-80-20, F-18-80-20, and F-22-80-20 revealed a progressive increase in ductility with larger SFCB bar diameters. The ductility increased from 5.33 in F-14-80-20 to 5.75 in F-18-80-20, representing a 7.88% improvement, and further to 5.92 in F-22-80-20, marking an additional 3.00% increase. This trend

demonstrated that increasing the SFCB bar diameter enhanced the columns' ability to undergo deformation before failure, leading to greater energy absorption and improved structural resilience. The ability to sustain larger strains before failure is particularly beneficial in seismic or cyclic loading conditions, where enhanced ductility reduces the risk of sudden brittle failure.

4.3. Effect of Axial Load on Ductility

The ductility of columns F-18-80-20, F-18-80-30, and F-18-80-40, which had axial load ratios of 20%, 30%, and 40%, respectively, decreased as the applied axial load increased. Specifically, the ductility of F-18-80-20 was 5.75, which declined to 5.25 in F-18-80-30, representing an 8.70% reduction, and further decreased to 5.00 in F-18-80-40, marking an additional 4.76% reduction. This decline in ductility under higher axial loads can be attributed to the increased compressive forces exerted on the columns, which accelerate the initiation and propagation of concrete cracking, thereby diminishing the material's ability to undergo plastic deformation. Additionally, higher axial loads elevate the risk of longitudinal reinforcement buckling, further compromising the structural integrity of the columns. The increased compressive stresses also reduce the effectiveness of confinement provided by the transverse reinforcement, leading to earlier concrete spalling and a significant reduction in energy absorption capacity. As a result, columns subjected to higher axial loads exhibit a more brittle failure mode, highlighting the critical influence of axial load levels on the ductility and overall performance of reinforced concrete columns.

4.4. Effect of Stirrup Spacing on Ductility

The ductility of columns F-18-80-20, F-18-100-20, and F-18-150-20, which had stirrup spacings of 80 mm, 100 mm, and 150 mm, respectively, decreased as the stirrup spacing increased. Specifically, the ductility of F-18-80-20 was 5.75, which declined to 5.50 in F-18-100-20, representing a 4.35% reduction, and further decreased to 5.25 in F-18-150-20, marking an additional 4.55% reduction. This reduction in ductility was primarily due to the diminished confinement effect of the concrete core as the stirrup spacing increased. Closer stirrup spacing provided more effective confinement, restricting lateral expansion of the concrete and delaying the onset of cracking. Furthermore, improved confinement helped prevent premature buckling of the longitudinal reinforcement, thereby enhancing the column’s ability to sustain larger deformations before failure. As a result, columns with wider stirrup spacing exhibited lower ductility and a reduced capacity to absorb energy, highlighting the importance of closely spaced stirrups in improving the overall structural performance and deformation capacity of reinforced concrete columns.

5. Cumulative Energy

The relationship between cumulative energy and drift ratio is a critical metric for evaluating the seismic performance of RC columns under cyclic loading. Cumulative energy, measured in kilonewton-meters (kN·m), represents the total energy absorbed by the column during deformation, while the drift ratio indicates the extent of lateral displacement relative to the column height. This relationship reflects the column's ability to dissipate energy through inelastic deformations, which is essential for mitigating damage during seismic events. A higher cumulative energy absorption at a given drift ratio indicates better performance, as the column can withstand larger displacements without significant loss of structural integrity [23]. This capability is vital for ensuring the safety and durability of structures during earthquakes.

5.1. Comparison of Steel and SFCB-Reinforced Columns

Column F-14-80-20 exhibited significantly superior energy absorption capacity compared to the steel-reinforced column S-10-80-20, as illustrated in Figure 10-a. Specifically, at a drift ratio of 2%, F-14-80-20 absorbed 75 kN·m of energy, which is 25% higher than the 60 kN·m absorbed by S-10-80-20. As the loading progressed to the point of failure, the energy absorption of F-14-80-20 increased to 100 kN·m, whereas S-10-80-20 absorbed only 65 kN·m. This represents a substantial 53.8% improvement in energy absorption for F-14-80-20 over its steel-reinforced counterpart. These findings suggest that F-14-80-20 demonstrates enhanced ductility and greater energy dissipation capacity, making it a more suitable choice for seismic applications, where structures must withstand large displacements and dissipate energy efficiently to maintain stability and integrity [24].

5.2. Effect of SFCB Bar Diameter on Energy Absorption

A comparison of columns F-14-80-20, F-18-80-20, and F-22-80-20, with bar diameters of 14 mm, 18 mm, and 22 mm, respectively, reveals significant improvements in energy absorption as the bar diameter increases, as shown in Figure 10-b. At a drift ratio of 2%, F-14-80-20 absorbed 75 kN·m, while F-18-80-20 absorbed 100 kN·m, marking a 33.33% increase. F-22-80-20 demonstrated even greater energy absorption, with 120 kN·m, representing a 60% increase over F-14-80-20. Upon reaching failure, F-14-80-20 absorbed 100 kN·m, F-18-80-20 absorbed 260 kN·m (a 160% increase), and F-22-80-20 absorbed 300 kN·m (a 200% increase). These results highlight that increasing the SFCB bar diameter significantly enhances energy dissipation, thereby improving the column's structural resilience and ductility under seismic loading.

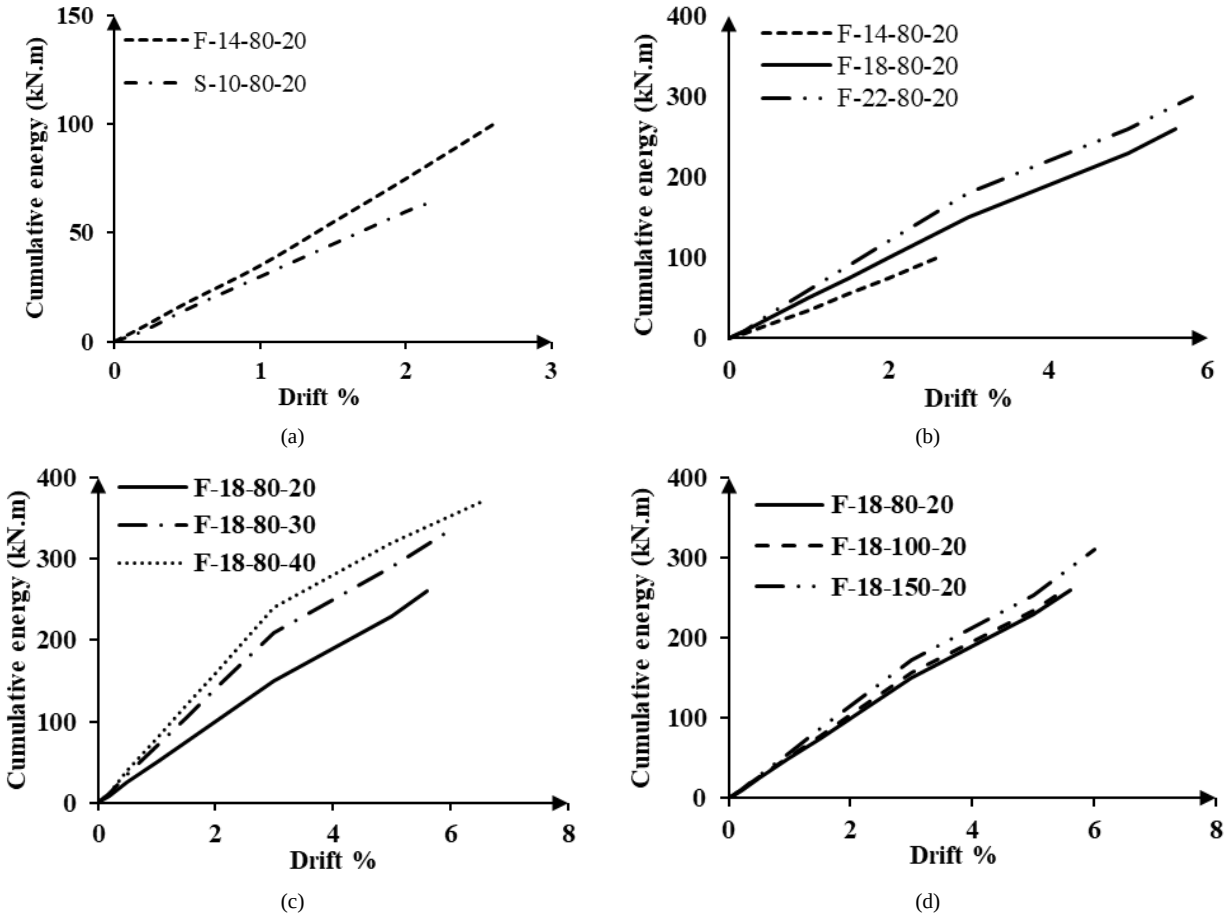

Figure 10. Cumulative energy vs drift ratio

5.3. Effect of Axial Load on Energy Absorption

Columns F-18-80-20, F-18-80-30, and F-18-80-40, with axial load ratios of 20%, 30%, and 40%, respectively, demonstrated an increase in energy absorption with higher axial loads, as shown in Figure 10-c. At a 2% drift ratio, F-18-80-20 absorbed 100 kN·m, while F-18-80-30 absorbed 140 kN·m, representing a 40% increase. F-18-80-40 absorbed 160 kN·m, a 60% increase compared to F-18-80-20. This trend underscores the fact that higher axial loads improve the column's energy dissipation capacity, enhancing its seismic performance. However, it is crucial to balance these benefits with the potential for earlier yielding and a reduced deformation capacity under very high loads, which may compromise the column's overall effectiveness in extreme seismic conditions [23].

5.4. Effect of Stirrup Spacing on Energy Absorption

Columns F-18-80-20, F-18-100-20, and F-18-150-20, with stirrup spacings of 80 mm, 100 mm, and 150 mm, respectively, exhibited increased energy absorption with wider tie spacing, as shown in Figure 10-d. At a 2% drift ratio, F-18-80-20 absorbed 100 kN·m, while F-18-100-20 absorbed 104 kN·m, representing a 4% increase. F-18-150-20 demonstrated the highest energy absorption among the three, reaching 115 kN·m, which corresponds to a 15% increase compared to F-18-80-20. Although wider tie spacing enhances energy absorption, the diminishing returns observed suggest that an optimal balance between tie spacing and energy dissipation should be carefully considered to prevent any compromise in structural integrity.

6. Columns' Rotations

The rotation of the columns at the failure stage is illustrated in Figure 11. The rotation percentages were calculated using data from LVDTs installed on the column faces perpendicular to the direction of lateral load application. These LVDTs measured displacement differences, which were then converted into rotation values in radians. By analyzing the displacement differences at various locations along the column, the total rotation was divided into three primary components: plastic hinge rotation, main crack rotation, and other components of rotation. To avoid double counting the contributions of the plastic hinge and main cracks, the LVDT data was carefully analyzed to separate localized deformations associated with main cracks from the overall deformations in the plastic hinge region. The contribution of each component to the total drift angle was determined by calculating the ratio of each rotation component to the total column drift angle. This method provides a comprehensive understanding of the deformation behavior of the columns under different loading and reinforcement conditions [15].

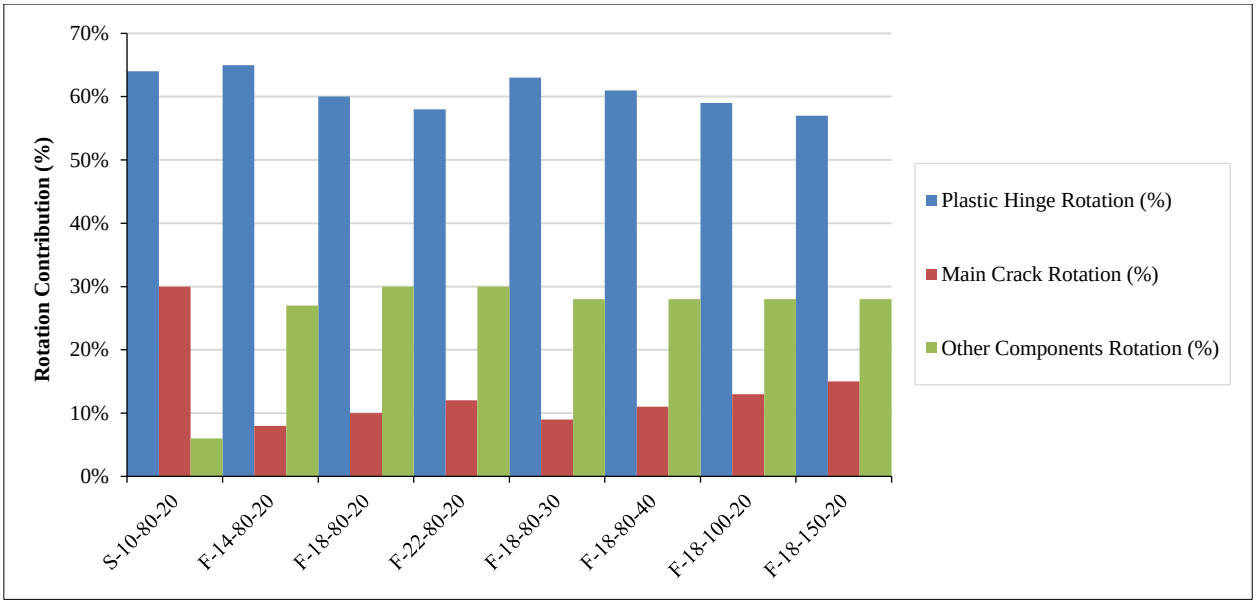

Figure 11. Columns' rotation at failure

6.1. Comparison of Steel and SFCB-Reinforced Columns

The performance of column F-14-80-20, reinforced with SFCB, was compared to that of the steel-reinforced column S-10-80-20. Both columns exhibited similar rotation percentages due to the development of the plastic hinge, with F-14-80-20 showing 65% rotation and S-10-80-20 showing 64%. However, the main crack rotation in S-10-80-20 was significantly higher at 30%, compared to only 8% in F-14-80-20. This suggests that more localized deformation occurred at the column-footing interface in the steel-reinforced specimen, while the SFCB reinforcement in F-14-80-20 mitigated this effect. The results indicate that SFCB reinforcement reduces localized cracking and helps distribute deformation more evenly throughout the column.

6.2. Effect of SFCB Bar Diameter on Rotation Components

A comparison of columns F-14-80-20, F-18-80-20, and F-22-80-20, with SFCB bar diameters of 14 mm, 18 mm, and 22 mm, respectively, demonstrates the influence of bar diameter on the rotation components. As the bar diameter increased from 14 mm to 22 mm, the plastic hinge rotation decreased slightly, from 65% in F-14-80-20 to 58% in F-22-80-20. In contrast, the main crack rotation exhibited a slight increase, indicating that larger bar diameters contribute to a marginally higher tendency for localized rotation at the base of the column. This analysis underscores the impact of bar diameter on the structural behavior of SFCB-reinforced columns, suggesting that while larger diameters may reduce overall plastic hinge rotation, they may also lead to more localized rotation at the column's base.

6.3. Effect of Axial Load on Rotation Components

Columns F-18-80-20, F-18-80-30, and F-18-80-40, with axial load ratios of 20%, 30%, and 40%, respectively, exhibited consistent rotation behavior across the different axial load conditions. The plastic hinge rotation remained stable, with only a slight increase from 60% in F-18-80-20 to 61% in F-18-80-40. Similarly, the main crack rotation showed minimal variation between these columns. This consistency suggests that changes in axial load have a negligible effect on both plastic hinge and main crack rotation, highlighting the robustness and reliability of SFCB-reinforced columns under varying axial loads.

6.4. Effect of Stirrup Spacing on Rotation Components

The influence of stirrup spacing on rotation components was evaluated by comparing columns F-18-80-20, F-18-100-20, and F-18-150-20, with stirrup spacings of 80 mm, 100 mm, and 150 mm, respectively. As the stirrup spacing increased, the plastic hinge rotation decreased slightly from 60% in F-18-80-20 to 57% in F-18-150-20, while the main crack rotation increased from 10% to 15%. This trend suggests that wider stirrup spacing reduces the contribution of the plastic hinge to the total rotation while increasing the role of main cracks in the deformation process. These findings emphasize the importance of selecting an appropriate stirrup spacing to effectively control deformation behavior and ensure the structural performance of SFCB-reinforced columns.

7. Strains in the Reinforcement

The strain versus drift ratio curves, shown in Figure 12, illustrate the response of each column under combined cyclic and axial loading. In general, as the drift ratio increases, the strain in the reinforcement also increases. Variations in the curves are influenced by factors such as material type, reinforcement diameter, stirrup spacing, and axial load. These factors collectively determine the column's ability to dissipate energy and withstand deformation, with higher strain values indicating greater stress and potential yielding in the reinforcement.

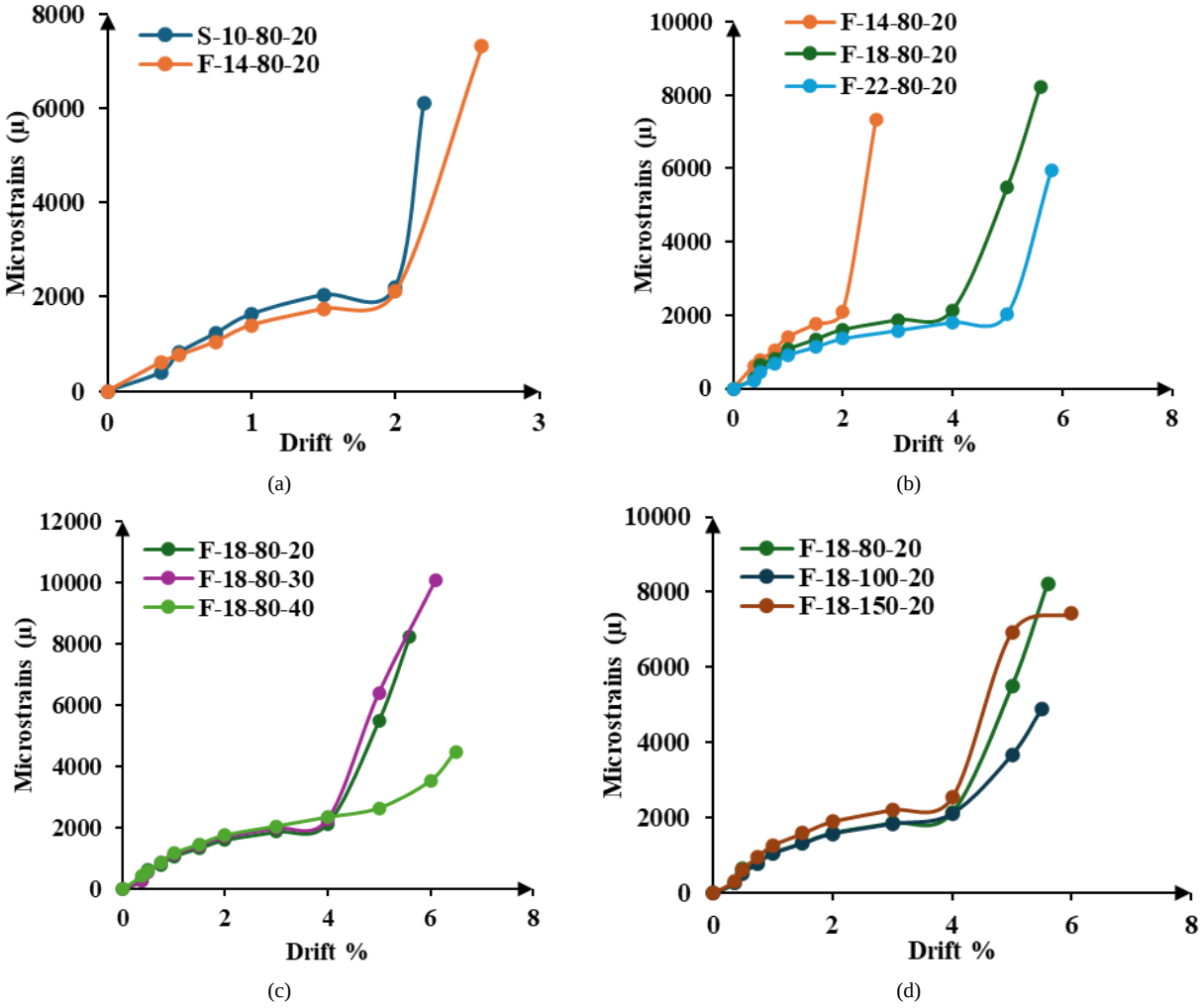

Figure 12. Bars' strains vs. drift ratio

7.1. Comparison of Steel and SFCB-Reinforced Columns

For the steel-reinforced column S-10-80-20, the strain reached approximately 2042.96 microstrain at a 1.5% drift ratio, as shown in Figure 12-a. In contrast, the SFCB-reinforced column F-14-80-20 exhibited a strain of around 1756.34 microstrain at the same drift ratio, which represents a 14% reduction compared to S-10-80-20. At a 2% drift ratio, F-14-80-20 reached approximately 2107.61 microstrain, indicating the onset of yielding, while S-10-80-20 had already exceeded the yielding point. These results demonstrate that SFCB reinforcement offers superior performance, exhibiting lower strains at comparable drift ratios and highlighting its enhanced structural capacity.

7.2. Effect of SFCB Bar Diameter on Strain

The influence of SFCB bar diameter on strain is clearly evident when comparing columns F-14-80-20, F-18-80-20, and F-22-80-20, as shown in Figure 12-b. Column F-18-80-20, with 18 mm bars, exhibited a strain of approximately 1335.55 microstrain at a 1.5% drift ratio, representing a 24% reduction compared to F-14-80-20. At a 2% drift ratio, F-18-80-20 showed a strain of 1602.66 microstrain, again a 24% reduction compared to F-14-80-20. Column F-22-80-20, with 22 mm bars, exhibited a strain of around 1355.67 microstrain at a 2% drift ratio, reflecting a 15% reduction compared to F-14-80-20. These findings underscore the beneficial effects of increasing reinforcement diameter, as larger bars lead to lower strains at similar drift ratios, thereby enhancing the structural performance of the columns.

7.3. Effect of Axial Load on Strain

The impact of axial load on strain is evident when comparing columns F-18-80-20, F-18-80-30, and F-18-80-40, as shown in Figure 12-c. Column F-18-80-20, with a 20% axial load, reached approximately 1602.66 microstrain at a 2% drift ratio. For F-18-80-30, with a 30% axial load, the strain increased to around 1712.43 microstrain at the same drift ratio, representing a 7% increase compared to F-18-80-20. At a 3% drift ratio, F-18-80-30 reached 1997.84 microstrain, while F-18-80-20 reached 1869.77 microstrain, again showing a 7% increase for F-18-80-30. Column F-18-80-40, with a 40% axial load, exhibited a strain of about 1763.47 microstrain at a 2% drift ratio, a 10% increase compared to F-18-80-20. At a 3% drift ratio, F-18-80-40 reached 2057.39 microstrain, reflecting a 9% increase compared to F-18-80-20. These results indicate that higher axial loads result in increased strains at similar drift ratios, suggesting that axial load plays a significant role in the strain behavior of reinforced columns.

7.4. Effect of Stirrup Spacing on Strain

The effect of stirrup spacing on strain is demonstrated by comparing columns F-18-80-20, F-18-100-20, and F-18-150-20, as shown in Figure 12-d. Column F-18-80-20, with 80 mm stirrup spacing, exhibited a strain of approximately 1602.66 microstrain at a 2% drift ratio. For F-18-100-20, with 100 mm stirrup spacing, the strain increased to around 1869.77 microstrain at the same drift ratio, reflecting a 17% increase compared to F-18-80-20. Column F-18-150-20, with 150 mm stirrup spacing, reached approximately 1997.84 microstrain at a 3% drift ratio, a 7% increase compared to F-18-80-20. These findings emphasize that wider stirrup spacing leads to higher strains and reduced structural performance, highlighting the importance of providing adequate confinement through closer stirrup spacing to improve the column's overall behavior under seismic loading.

8. Design Drift Ratio According to International Standards

Since there are no established standards specifically for SFCB-reinforced columns, their performance was evaluated using international standards for steel-RC and FRP-RC structures. American, Canadian, and European seismic design standards prescribe specific design drift ratios to ensure buildings can withstand seismic events while maintaining structural integrity.

- American Standards: The ASCE/SEI 7-16 standard [25] recommends a maximum drift ratio of 2.5% for ordinary moment-resisting frames and 2.0% for special moment-resisting frames. Similarly, the ACI 318-19 guidelines [26] align with these recommendations for concrete structures.
- Canadian Standards: The CSA S806-12 standard [27] specifies a design drift ratio of either 2.5% or 4.0%, depending on the structural type and significance. The CSA A23.3-19 [28] and NBCC 2015 [29] standards generally recommend a drift ratio of up to 2.5% for typical buildings, with stricter limits for critical structures.
- European Standards: Eurocode 8 (EN 1998) [30] recommends drift ratios of up to 1.5% for ordinary moment-resisting frames, with more stringent criteria for special structures based on their importance and height.

8.1. Comparison with Tested Columns

The performance of the tested columns was compared against these international standards, revealing significant insights:

1. **Steel-Reinforced Column (S-10-80-20)**: This column achieved a maximum drift ratio of 2.2%, which falls within the acceptable range for ASCE/SEI 7-16 [25] and ACI 318-19 [26] (2.5%) but exceeds the Eurocode 8 limit of 1.5% [30].
2. **SFCB-Reinforced Column (F-14-80-20)**: With a maximum drift ratio of 2.6%, this column slightly exceeded the ASCE/SEI 7-16 [25] and ACI 318-19 [26] limits. This indicates an enhanced capacity to handle more significant seismic events, suggesting improved resilience.
3. **Other SFCB-Reinforced Columns (F-18-80-20, F-22-80-20, F-18-80-30, F-18-80-40, F-18-100-20, and F-18-150-20)**: These columns demonstrated even greater performance, with maximum drift ratios ranging from 5.5% to 6.5%. These values far exceed the typical limits set by international standards, showcasing their robust ability to endure higher levels of seismic activity. While standards generally cap the drift ratio at 2.5%, 4.0%, or 1.5%, depending on the guideline, exceeding these limits can be seen as a positive indicator of structural strength and flexibility. A visual representation of these results is provided in Figure 13.

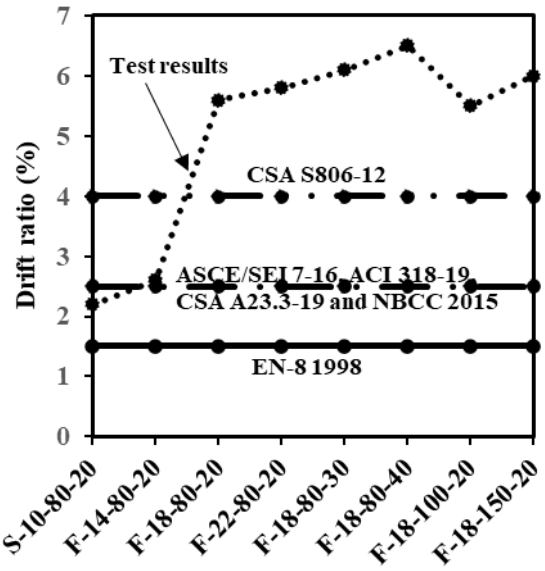

Figure 13. Drift ratio according to different standards

8.2. Implications for Seismic Design

The performance of the SFCB-reinforced columns, which surpassed the recommended drift ratios set by American, Canadian, and European seismic design standards, highlights their superior resilience to seismic events. This robustness ensures safety and structural integrity even under extreme conditions, providing an additional layer of confidence in their seismic performance. These findings suggest that SFCB-reinforced columns are well-suited for applications requiring high seismic resilience, offering a viable alternative to traditional steel and FRP reinforcement.

8.3. Comparison with Existing Literature

Limited research has examined the lateral behavior of SFCB-RC columns. Such as, Sun et al. (2025) [11] investigated circular columns reinforced with partially unbonded SFCBs and hybrid stirrups, highlighting the influence of unbonded length, post-yield stiffness, and core confinement. Their findings showed that increasing the unbonded length (up to 450 mm) and the level of confinement significantly improved post-yield stiffness ratios (up to 6.54%) and ductility, with columns sustaining drift ratios of up to 6.0%.

The current study focused on square columns subjected to combined cyclic and axial loading, examining the effects of varying SFCB diameters (14–22 mm), axial load ratios (20–40%), and stirrup spacing (80–150 mm). It found that larger SFCB diameters enhanced peak load capacity by up to 20% and increased drift ratios to as much as 6.5%, while higher axial loads and wider stirrup spacing reduced ductility by up to 13.46% and 8.90%, respectively.

Both studies—Sun et al. (2025) [11] and the present work—demonstrate the superior performance of SFCB-reinforced columns compared to traditional steel-reinforced ones, particularly in terms of energy dissipation and seismic resilience. While Sun et al. (2025) [11] emphasized the advantages of debonding and confinement in enhancing post-yield stiffness and deformation capacity, the current study highlights the critical roles of bar diameter and axial load in influencing ductility and drift. Notably, the columns tested in this study achieved higher drift ratios (up to 6.5%) than those in the Sun et al. (2025) [11] study, suggesting that SFCBs are effective in both deformation capacity and stiffness control. Collectively, these findings confirm that SFCBs represent a promising alternative for seismic design, with performance that can be optimized through geometric and material parameters.

9. Conclusions

The experimental study on SFCB-reinforced RC columns under combined cyclic and axial loading yielded the following key conclusions:

- *Superior Energy Absorption*: SFCB-reinforced columns demonstrated significantly higher energy absorption compared to traditional steel-reinforced columns. For instance, column F-14-80-20 absorbed 100 kN·m of energy at failure, outperforming the steel-reinforced column S-10-80-20, which absorbed only 65 kN·m. This represents a 53.8% improvement in energy absorption, highlighting the enhanced performance of SFCB reinforcement.
- *Impact of Bar Diameter*: Increasing the diameter of SFCB bars improved the ductility and drift ratio of the columns. The ductility increased from 5.33 in F-14-80-20 to 5.75 in F-18-80-20 (a 7.88% improvement) and further to 5.92 in F-22-80-20 (a 3.00% improvement). These results indicate that larger SFCB diameters contribute significantly to enhanced ductility and energy absorption, making the columns more resilient under cyclic loading.

- *Impact of Axial Load*: Higher axial loads enhanced the energy absorption capacity of SFCB-reinforced columns. For example, column F-18-80-40 absorbed 60% more energy than F-18-80-20 at a 2% drift ratio. However, ductility decreased with increasing axial loads, dropping from 5.75 in F-18-80-20 to 5.00 in F-18-80-40 (a 13% reduction). This suggests a trade-off between energy absorption and ductility under higher axial loads.
- *Effect of Stirrup Spacing*: Wider stirrup spacing reduced the ductility of SFCB-reinforced columns. The ductility decreased from 5.75 in F-18-80-20 to 5.50 in F-18-100-20 (a 4.35% reduction) and further to 5.25 in F-18-150-20 (a 4.55% reduction). Closer stirrup spacing improved concrete confinement and energy dissipation capacity, emphasizing the importance of adequate transverse reinforcement.
- *Rotation Behavior*: The plastic hinge rotation in SFCB-reinforced columns remained consistent across the tested parameters and was comparable to that of steel-reinforced columns. This suggests that SFCB reinforcement has minimal impact on rotational behavior while maintaining overall structural integrity.
- *Seismic Performance*: SFCB-reinforced columns exceeded the drift ratios recommended by international standards, including ASCE/SEI 7-16, ACI 318-19, CSA S806-12, and Eurocode 8. These columns maintained structural integrity under high drift ratios, demonstrating their suitability for seismic applications.

These findings highlight the superior performance of SFCB-reinforced RC columns, particularly in terms of energy absorption, ductility, and seismic resilience. The results suggest that SFCB reinforcement offers a viable and preferable alternative to traditional steel and FRP reinforcement, especially in seismic-prone regions.

10. Declarations

10.1. Author Contributions

Conceptualization, M.H.A. and A.G.; methodology, O.F.N.; formal analysis, O.F.N.; investigation, A.M.A.; resources, M.H.A.; data curation, H.M.E.S.I.; writing—original draft preparation, O.F.N.; writing—review and editing, I.T.M.; visualization, I.T.M.; supervision, M.H.A.; project administration, A.G. All authors have read and agreed to the published version of the manuscript.

10.2. Data Availability Statement

The data presented in this study are available on request from the corresponding author.

10.3. Funding

The authors received no financial support for the research, authorship, and/or publication of this article.

10.4. Acknowledgements

The authors extend their gratitude to the Department of Civil Engineering, Faculty of Engineering – Mataria, Helwan University, and the Housing and Building National Research Center (HBRC) for providing essential facilities and support that enabled the successful completion of this research.

10.5. Conflicts of Interest

The authors declare no conflict of interest.

11. References

[1] ACI 440.11-22. (2022). Building code requirements for structural concrete reinforced with Glass Fiber-Reinforced Polymer (GFRP) bars—code and commentary. American Concrete Institute (ACI), Michigan, United States.

[2] Cairns, J., Dut, Y., & Law, D. (2008). Structural performance of corrosion-damaged concrete beams. Magazine of Concrete Research, 60(5), 359–370. doi:10.1680/macr.2007.00102.

[3] Gouda Sayed, A., H. Ali, A., & M. Mohamed, H. (2022). Innovative FE Analysis to Investigate the Effect of Flexural Reinforcement on the Behavior of Beams. International Journal of Green Management and Business Studies, 2(2), 41–52. doi:10.56830/qkul4110.

[4] Hassan, G. B., Al-Kamaki, Y. S. S., Mohammed, A. A., & AlSaad, A. (2023). Long-term exposure of RC columns immersed in seawater or crude oil confined with CFRP fabrics under monotonic or cyclic loading. Case Studies in Construction Materials, 18. doi:10.1016/j.cscm.2022.e01747.

[5] Windisch, A. (2010). Performance evaluation of glass fiber-reinforced polymer shear reinforcement for concrete beams. ACI Structural Journal, 107(6), 738–740. doi:10.14359/51663388.

[6] Manalo, A., Maranan, G., Benmokrane, B., Cousin, P., Alajarmeh, O., Ferdous, W., Liang, R., & Hota, G. (2020). Comparative durability of GFRP composite reinforcing bars in concrete and in simulated concrete environments. Cement and Concrete Composites, 109, 103564. doi:10.1016/j.cemconcomp.2020.103564.

[7] Ali, A. H., Gouda, A., Mohamed, H. M., & Esmael, H. M. (2022). Experimental and Numerical Analysis of Steel and Fiber-Reinforced Polymer Concrete Beams under Transverse Load. ACI Structural Journal, 119(4), 109–121. doi:10.14359/51734651.

[8] De Luca, A., Matta, F., & Nanni, A. (2010). Behavior of full-scale glass fiber-reinforced polymer reinforced concrete columns under axial load. ACI Structural Journal, 107(5), 589–596. doi:10.14359/51663912.

[9] Etman, E. E., Mahmoud, M. H., Hassan, A., & Mowafy, M. H. (2023). Flexural behaviour of concrete beams reinforced with steel-FRP composite bars. Structures, 50, 1147–1163. doi:10.1016/j.istruc.2023.02.098.

[10] Wu, G., Sun, Z., Wu, Z., & Luo, Y. (2012). Mechanical properties of steel-FRP composite bars (SFCBs) and performance of SFCB reinforced concrete structures. Advances in Structural Engineering, 15(4), 625–636. doi:10.1260/1369-4332.15.4.625.

[11] Sun, Y., Sun, Z., Zheng, Y., Yao, L., Cai, X., & Ibrahim, A. I. (2025). Lateral behavior of circular concrete columns reinforced with partially unbonded steel basalt-fiber composite bars and hybrid stirrups. Engineering Structures, 332, 120051. doi:10.1016/j.engstruct.2025.120051.

[12] Huang, Z., Chen, W., Hao, H., Siew, A. U., Huang, T., Ahmed, M., & Pham, T. M. (2024). Lateral impact performances of geopolymer concrete columns reinforced with steel-BFRP composite bars. Construction and Building Materials, 411, 134411. doi:10.1016/j.conbuildmat.2023.134411.

[13] Ge, W., Zhang, S., Zhang, Z., Guan, Z., Ashour, A., Sun, C., Lu, W., & Cao, D. (2023). Eccentric compression behavior of Steel-FRP composite bars RC columns under coupling action of chloride corrosion and load. Structures, 50, 1051–1068. doi:10.1016/j.istruc.2023.02.090.

[14] Xu, L., Wang, X., Dong, B., Yang, X., & Pan, J. (2024). Seismic behaviors of steel-FRP composite bar-reinforced engineered cementitious composites columns under reversed cyclic loads. Engineering Structures, 316(1), 118571. doi:10.1016/j.engstruct.2024.118571.

[15] Ali, M. A., & El-Salakawy, E. (2016). Seismic Performance of GFRP-Reinforced Concrete Rectangular Columns. Journal of Composites for Construction, 20(3), 1–12. doi:10.1061/(asce)cc.1943-5614.0000637.

[16] ASTM D7205/D7205M-06. (2011). Standard Test Method for Tensile Properties of Fiber Reinforced Polymer Matrix Composite Bars. ASTM International, Pennsylvania, United States. doi:10.1520/D7205_D7205M-06.

[17] ASTM C39/C39M-21. (2023). Standard Test Method for Compressive Strength of Cylindrical Concrete Specimens. ASTM International, Pennsylvania, United States. doi.10.1520/C0039_C0039M-21.

[18] Alsayed, S. H. (1998). Flexural behaviour of concrete beams reinforced with GFRP bars. Cement and Concrete Composites, 20(1), 1–11. doi:10.1016/s0958-9465(97)00061-9.

[19] Jeddian, S., Ghazi, M., & Sarafraz, M. E. (2024). Experimental study on the seismic performance of GFRP reinforced concrete columns actively confined by AFRP strips. Structures, 62, 106248. doi:10.1016/j.istruc.2024.106248.

[20] Sharbatdar, M. K. (2003). Concrete columns and beams reinforced with FRP bars and grids under monotonic and reversed cyclic loading. Ph.D. Thesis, University of Ottawa, Ottawa, Canada.

[21] Ozcebe, G., & Saatcioglu, M. (1987). Confinement of Concrete Columns for Seismic Loading. ACI Structural Journal, 84(4), 308–315. doi:10.14359/1660.

[22] Abbasnia, R., Ahmadi, R., & Ziaadiny, H. (2012). Effect of confinement level, aspect ratio and concrete strength on the cyclic stress-strain behavior of FRP-confined concrete prisms. Composites Part B: Engineering, 43(2), 825–831. doi:10.1016/j.compositesb.2011.11.008.

[23] Park, R., & Paulay, T. (1991). Reinforced concrete structures. John Wiley & Sons, Hoboken, United States.

[24] Chopra, A. K. (2017). Dynamics of Structures: Theory and applications to earthquake engineering. Pearson, London, United Kingdom.

[25] ASCE/SEI 7-16. (2016). Minimum design loads and associated criteria for buildings and other structures. American Society of Civil Engineers, Reston, United States. doi:10.1061/9780784414248.

[26] ACI 318-19. (2019). Building Code Requirements for Structural Concrete (ACI 318-19) and Commentary (ACI 318R-19). American Concrete Institute (ACI), Farmington Hills, United States.

[27] CSA S806-12. (2012). Design and construction of building structures with fiber-reinforced polymers. Canadian Standards Association, Toronto, Canada.

[28] CSA A23.3-19. (2019). Design of concrete structures. Canadian Standards Association, Toronto, Canada.

[29] National Research Council Canada. (2015). National Building Code of Canada. National Research Council Canada, Ottawa, Canada.

[30] EN 1998-1. (2004). Eurocode 8: Design of structures for earthquake resistance. European Committee for Standardization, Brussels, Belgium.